The significance of engulfment in the process of turbulent entrainment by plumes

H. C. Burridge[1,2], D. A. Parker[1], E. S. Kruger[1], J. L. Partridge[1] and P. F. Linden[1]

[1]Department of Applied Mathematics and Theoretical Physics, University of Cambridge.
[2]Department of Civil and Environmental Engineering, Imperial College London.
hcb39@cam.ac.uk

Abstract

We present simultaneous two-dimensional velocity and scalar concentrations measured on a central vertical plane in a turbulent plume. We use an edge-detection algorithm to determine the scalar plume edge, and compare the data obtained in both a fixed Eulerian frame and relative to local plume coordinates defined in terms of the instantaneous plume edge. We observe that the time-averaged distributions of vertical and horizontal velocity are self-similar. Measurements in the plume coordinate show that there is significant vertical flow outside the edge of the plume, contrary to the classical notion of purely horizontal velocities at the plume edge. We observe large variations in the plume width and reason these to be due to the passage of large coherent eddies. The flow within the plume and in the nearby ambient fluid depends on whether an eddy is present or absent. When an eddy is present and the plume is wide, the vertical velocities near the plume edge are small, but in regions where the plume is narrow and there is no eddy, large vertical velocities are observed outside the plume.

1 Introduction

Turbulent plumes are of significance to the environment and the economy. For example, in 2010 plumes produced by the eruption of the Icelandic volcano *Eyjafjallajökull* and the *Deepwater Horizon* oil leak in the Gulf of Mexico had huge environmental impacts and very large economic consequences. The impact of such events and the ultimate fate of the plume fluid, often containing pollutants or contaminants, is largely determined by turbulent entrainment into the plume. The focus of this study is to examine the mechanisms responsible for turbulent entrainment through an experimental investigation of saline plumes in a freshwater environment.

We consider a pure plume produced by a steady localised source of buoyancy within a quiescent environment of uniform density. Plumes induce a flow within the surrounding ambient fluid that is typically considered (e.g. Morton et al., 1956) to be predominately horizontal. By making simultaneous measurements of the flow velocities (using particle image velocimetry, PIV) and the scalar edge (using light induced fluorescence, LIF) of high Péclet number saline plumes we show that this is not the case. Indeed, we show that vertical velocities at, and outside, the edge of the plume are significant, and that entrainment of ambient fluid is caused by engulfment by large scale eddies.

2 Experiments

The experiments were performed in a glass tank of horizontal cross-section 100 cm x 80 cm filled with dilute saline solution (of uniform density ρ_a) to a depth of 85 cm. Relatively

dense source fluid was supplied via an apparatus providing a constant gravitational head, thereby ensuring a steady flow, to a plume nozzle, of radius $r_0 = 0.25$cm. The source fluid was an aqueous saline (NaCl) solution of density ρ_0 with reduced gravity (buoyancy) at the source in the range $73.4\,\mathrm{cm/s^2} \leq g_0' \equiv g(\rho_0 - \rho_a)/\rho_a \leq 76.9\,\mathrm{cm/s^2}$. Three experimental plumes were analysed, two of which were of notionally identical source conditions in order to assess the repeatability of the experiments. We collected data within a vertical region sufficiently far from the source so that the plumes were both fully turbulent and were notionally pure, i.e. the plumes had attained an invariant balance between inertia and buoyancy.

In order to obtain simultaneous measurements of the scalar edge of the plumes we added a small quantity (approximately $5 \times 10^{-7}\,\mathrm{g/cm^3}$) of sodium fluorescein to the source saline solution in order to stain the source plume fluid. Lighting the central plane within the plume, we recorded images of both the light emitted by the fluorescein and that reflected by the PIV particles. Given that the molecular diffusivity of the dye (sodium fluorescein) and the buoyancy scalar (sodium chloride) are similar and that the flow was high Péclet number ($\mathrm{Pe} \approx 3 \times 10^6$) we could be certain that by tracking the light emitted by the fluorescein we were tracking the location of the plume buoyancy scalar.

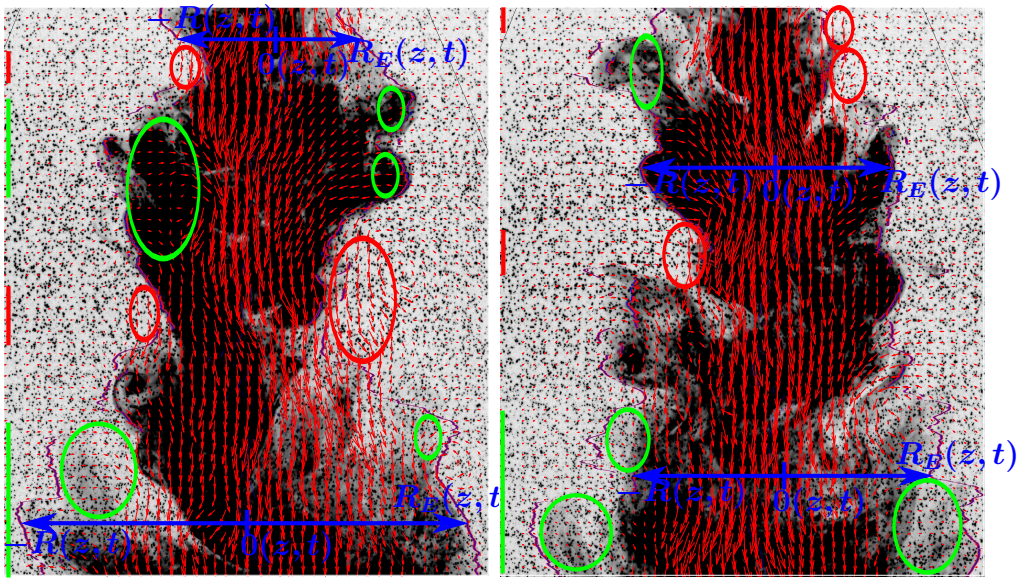

Figure 1: Two typical experimental images of a plume. The small dark 'spots' throughout both images are the 50 μm particles used to obtain PIV measurements. Dense 'plume fluid', stained by dye, is indicated by dark regions in each image. The edges detected by two independent algorithms are marked by the red solid lines (7 pixels wide) and blue solid lines (3 pixels wide). Velocity vectors (red arrows) indicate the local velocities within the fluid. Notice that where large-scale eddies are locally present the vertical velocities are small just outside and inside the plume edge (circled in green). At the locations where eddies are locally absent the vertical velocities outside the plume are significant (circled in red). The heights at which the measurement of the local width R_p indicate that large-scale coherent structures are present and absent are indicated by coloured bars (green present, red absent) on the left-hand edges of the two images.

3 Results

To provide new insights into the process of entrainment by plumes we examine the velocities in a coordinate system which follows the plume as it fluctuates in width and

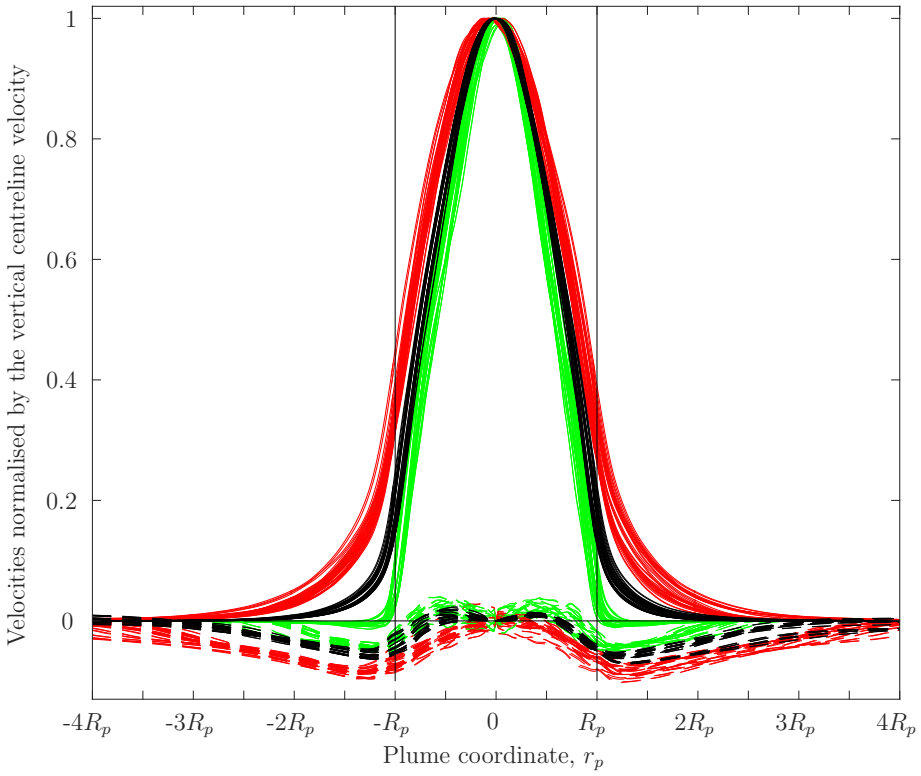

Figure 2: Vertical (solid lines) and horizontal (dashed lines) velocities averaged in the plume coordinate system, r_p. The full time-averaged velocities, $\overline{w_p}$ and $\overline{u_p}$, are marked in black; average velocities when eddies are present, $\overline{w_e}$ and $\overline{u_e}$, are marked in green; average velocities when no eddies are present, $\overline{w_n}$ and $\overline{u_n}$, are marked in red. The data from three different plumes at 18 different heights exhibit a broad collapse indicating self-similarity. Crucially the vertical velocities outside the plume are significant and are, indeed, greater than the horizontal velocities outside the plume.

meanders. At each time and height, we defined a local coordinate system in which the centreline position, denoted by $0(z,t)$, was defined as the instantaneous mid point of the edges from the scalar field at that height. We then record the velocities in a plume coordinate system $r_p(z,t)$, in which $r_p(z,t) = -R_p(z,t)$, $r_p(z,t) = 0(z,t)$ and $r_p(z,t) = R_p(z,t)$ denote the instantaneous left-hand edge, mid point and right-hand edge of the plume, respectively. Using this plume coordinate system the velocity data were then time-averaged to obtain the vertical velocity $\overline{w_p}$ and horizontal velocity $\overline{u_p}$. These data are plotted as the black curves in figure 2. The figure shows data from the three different plumes at 18 different heights and with the plume coordinate system calculated from two independent edge-detection algorithms. To our knowledge, this is the first time that velocity data for either jets or plumes have been conditionally averaged in this manner, *cf.* Westerweel et al. (2009) and Mistry et al. (2016).

The data averaged in this way collapse onto a single curve showing that the velocities are self-similar when viewed in plume coordinates. Crucially, the average vertical velocities at the plume edge (solid black lines at $\{-R_p, R_p\}$) are significant, and almost 20% of the velocities on the centreline. Such a finding is at odds with the classical view of a plume (Morton et al., 1956) in which the vertical velocities outside the plume were zero. Similarly significant vertical velocities at the plume edge were also observed by the recent study (Burridge et al., 2016) in which visible coherent structures were tracked using a cross-correlation technique. These structures at the plume edge (found to be of width $\sim 0.4R_p$) travelled at approximately 30% of the centreline velocities, similar to the velocities just

inside of the plume edge shown in figure 2.

Measurements of the horizontal velocities $\overline{u_p}$, marked by black dashed curves within figure 2, show radially inward (negative) velocities of increasing magnitude approaching the plume edge. Within the plume the magnitude of the (negative) radial velocities decreases rapidly, becomes positive (indicating a radially outward flow) and then approaches zero on the centreline. This reversal in the radial direction of the flow has been observed in jets (figures 13 and 11 in Westerweel et al., 2009; Mistry et al., 2016, respectively). Indeed, for both jets and plumes a change of sign in the radial flow can be explained by the fact that the vertical velocities in the flow decrease in the axial direction (most significantly near the centreline), and continuity thereby requires an outward radial flow locally.

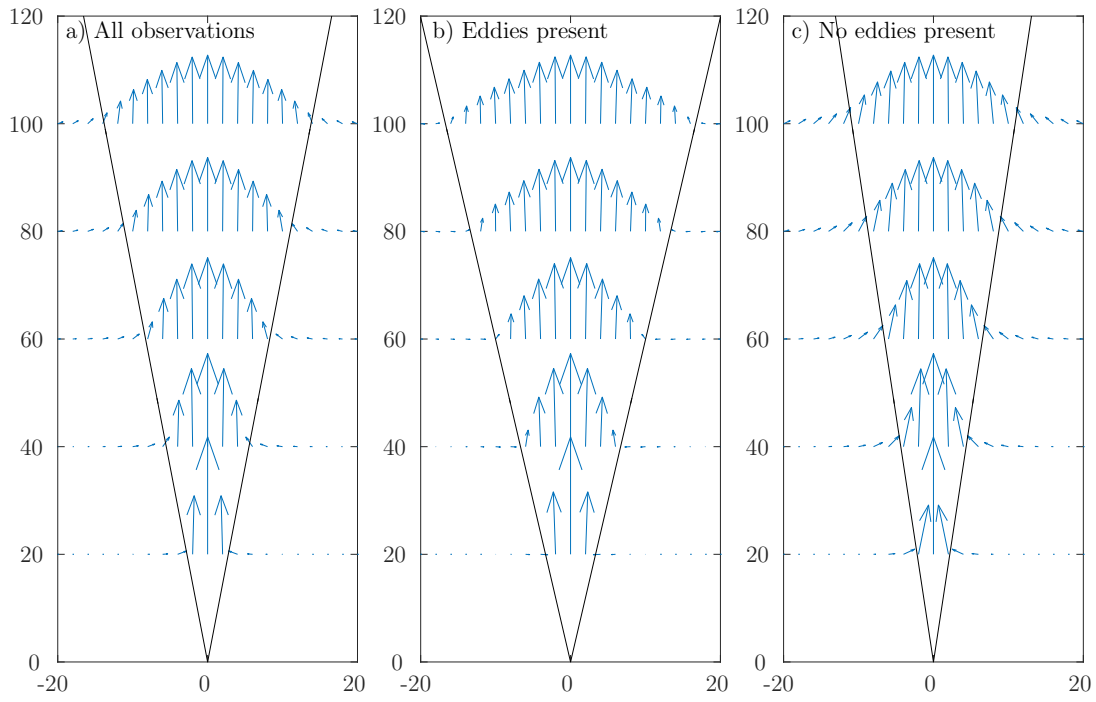

Figure 3: Time averaged views of a turbulent plume: a) all observations, b) observations when eddies are present, c) when eddies are absent. The black lines mark the time averaged position of the edge of the plume scalar field in each of the three states. The (blue) arrows mark the magnitude and direction of the measured velocity vectors (ensemble averaged over the 18 heights shown in figure 2). The axis are marked in arbitrary units.

3.1 Plume properties when eddies are present and absent

We now examine the plume properties and compare how they vary from the mean depending on whether one might reasonably expect a large-scale coherent structure (eddy) to be locally present or absent at a given height. To do so we recalculate the velocities conditioned on the presence or absence of a large scale eddy, by constructing time series at a particular height containing only times t_e at which large-scale eddies are locally present at that height. We reason that the presence of a large-scale coherent structure (eddy) results in an increase in the local width of the flow — as has been successfully used to track these structures in other studies (Burridge et al., 2016). The presence of an eddy within the plume is inferred when the local plume width is greater than the mean plume width by more than one standard deviation, $\sigma_R(z)$; i.e. $R_P(z,t_e) \geq R_p(z) + \sigma_R(z)$.

Conversely, we construct a time series containing times t_n when no large-scale eddies are present; i.e. when $R_P(z,t_n) \leq R_p(z) - \sigma_R(z)$. Again in the plume coordinate system we denote, for example, the mean vertical velocities, when large-scale eddies are present by $\overline{w_e}$ and when eddies are absent by $\overline{w_n}$.

The data for the velocities when eddies are present (green curves) and absent (red curves) are plotted in figure 2. As is the case for the ensemble data, these conditional data exhibit a broad collapse for each state, showing that the plume statistics are self-similar in all three states when viewed in the plume coordinate r_p.

When an eddy is present, the vertical velocities at the plume edge are *smaller* by about a factor of four compared to the mean and by about a factor of ten compared to when an eddy is absent. Horizontal velocities, on the other hand, are *larger* by about a factor of four when an eddy is present compared with when it is absent. When an eddy is present (green curves), the angle increases rapidly from close to horizontal ($0°$) just outside the plume edge to being close to vertical ($\sim 90°$) just within the plume edge. The velocity data for the events when there are no eddies locally present look very different (red curves), with observations of the vertical velocities at the plume edge being almost 35–45% of the centreline velocities.

Taking the data for the horizontal and vertical velocities in the plume co-ordinate, r_p, and knowing the time-averaged position of the plume edge $\overline{R_p}$ enables us to reconstruct the velocity field induced by and within a plume, relative to the scalar edge of the plume. These data are plotted in figure 3a and we note that the data from a simple Eularian view of the plume would look notionally identical. The figure shows that ambient fluid outside the scalar edge is drawn towards the plume, by the process of turbulent entrainment, but that as part of this process significant vertical velocity is induced within the ambient fluid before reaching the edge of the plume. The role that coherent structures play in this process is indicated by comparing equivalent reconstructions of the velocity field using data from observations when one can expect large-scale eddies to be present or absent, figures 3b and 3c, respectively. When eddies are present, the velocities within the (relatively wide) plume are almost entirely vertical and the flow outside predominately horizontal. Conversely, when eddies are absent the velocities within the (relatively thin) plume show a marked component of horizontal velocity well within the scalar edge and the ambient fluid far outside the scalar edges exhibits a significant component of vertical velocity.

Physically, a plume is never in a state of having either eddies present or absent throughout its height, quite the contrary is typical. At any given instant, a plume typically exhibits an alternating pattern of eddies being locally present and absent throughout its height. See, for example, the images in figure 1. With such a vision of a plume in mind, figures 3b and 3c illustrate that between large-scale coherent structures, vertical momentum is imparted (presumably by pressure gradients) to pockets of ambient fluid that are, in a relative sense, quite close to the plume centreline. The vertical momentum of these pockets of ambient fluid enable them to be engulfed into the plume more easily, providing a source for the flux of engulfed fluid, which we measured to be approximately 15% of the volume flux within the plume.

Such findings are significant since not only are they at odds with the classical notion of purely horizontal velocities outside the plume (Morton et al., 1956) but, moreover, they suggest that ambient fluid is being accelerated vertically long before reaching the plume edge. The relatively long-range acceleration of ambient fluid cannot be as a result of viscous effects at the plume edge and must result from relatively long-range pressure

gradients. Hence, the process of turbulent entrainment must, at the initial engulfment stage, be driven by these pressure gradients and not by viscous effects at the plume edge (*cf.* Westerweel et al., 2009). Such a view of entrainment is entirely akin to the view of entrainment expressed by Philip et al. (2014) for turbulent boundary layers and by Mistry et al. (2016) for turbulent (non-buoyant) jets.

4 Conclusions

Simultaneous measurements of the velocity field and the scalar edge of a plume have shown significant vertical velocities exist outside the plume. Velocities beyond the plume edge cannot be induced by viscous effects at the plume edge and must be induced by relatively long-range pressure gradients.

Examining our measurements when we expect large-scale coherent structures to be either present or absent has highlighted substantial differences in the velocity field in the two cases and we conclude that the passage of large-scale eddies at the plume edge drives pockets of ambient fluid at significant vertical velocities. The vertical momentum induced within these pockets of ambient fluid enable it to be engulfed within the plume thereby forming a significant part of the process of turbulent entrainment. We conclude that the engulfment of ambient fluid by large-scale eddies at the plume edge constitutes a significant part of the process of turbulent entrainment by plumes.

The authors gratefully acknowledge the skills and expertise provided by the technical staff of the G. K. Batchelor laboratory. This work was supported, in part, by the Leverhulme Trust Research Programme Grant RP2013-SL-008, the EPSRC Programme Grant EP/K034529/1, and by iCASE awards from NERC and the UK Met Office (RG82562), and EPSRC and Arup (RG83017).

References

Burridge, H. C., Partridge, J. L., and Linden, P. F. 2016. The fluxes and behaviour of plumes inferred from measurements of coherent structures within images of the bulk flow. *Atmos.-Ocean*, iFirst:1–15, Doi = 10.1080/07055900.2016.1175337.

Mistry, D., Philip, J., Dawson, J. R., and Marusic, I. 2016. Entrainment at multi-scales across the turbulent/non-turbulent interface in a turbulent jet. *J. Fluid Mech.*, Under Consideration

Morton, B. R., Taylor, G., and Turner, J. S. 1956. Turbulent gravitational convection from maintained and instantaneous sources. *Proc. R. Soc. Lond. A*, 234:1–23.

Philip, J., Meneveau, C., de Silva, C. M., and Marusic, I. 2014. Multiscale analysis of fluxes at the turbulent/non-turbulent interface in high Reynolds number boundary layers. *Phys. Fluids*, 26(1):015105.

Westerweel, J., Fukushima, C., Pedersen, J., and Hunt, J. C. R. 2009. Momentum and scalar transport at the turbulent/non-turbulent interface of a jet. *J. Fluid Mech.*, 631:199–230.